A new adaptation phase for thresholds in a CBR system associated to a region growing algorithm to segment tumoral kidneys

Florent Marie[1], Julien Henriet[1], and Jean-Christophe Lapayre[1]

FEMTO-ST Institute
Univ. Bourgogne-Franche-Comté, CNRS
DISC, 16 route de Gray, 25030 Besançon, France
{florent.marie, julien.henriet, jean-christophe.lapayre}@univ-fcomte.fr

Abstract. Image segmentation is an abundant topic for computer vision and image processing. Most of the time, segmentation is not fully automated, and a user is required to guide the process in order to obtain correct results. Yet, even with programs, it is a time-consuming process. In a medical context, segmentation can provide a lot of information to surgeons, but since this task is manual, it is rarely executed because of time. Artificial Intelligence (AI) is a powerful approach to create viable solutions for automated treatments. In this paper, we reused a case-based reasoning (CBR) system previously developed to segment renal parenchyma with a region growing algorithm and we completed its adaptation phase allowing a better adjustment of parameters before segmentation. Compared to the previous system, we added an adaptation for the thresholds values in addition to the adaptation of the seeds coordinates. We compared several versions of our new adaptation in order to determine the best and we confronted it with a deep learning approach realized in similar conditions.

Keywords: Case-Based Reasoning · Convolution Neural Network · segmentation · cancer tumour · healthcare imaging · artificial intelligence

1 Introduction

Nephroblastoma, also called Wilms tumour, is one of the most frequent abdominal tumours observed in young children, representing 5 to 14% of malignant paediatric tumours, and affects kidney. Because of tumour's presence, the kidney can be very deformed and hard to segment. Radiologists and surgeons need 3-Dimensional (3D) representations of the tumour and the border organs in order to establish the diagnosis and to plan the surgery

Segmentation is one of the key steps in the construction of such a 3D representation. During this process, each pixel of all scans has to be affected to one and only one region. Each region represents a given structure (right or left kidney, medullas, tumours, muscles, veins, cavities, etc.). The problem resides in the unforeseeable nature of the situation of the kidneys and radiologists and

surgeons must lead and verify the segmentations of more than 200 scans manually for each patient in order to improve the therapy, which, in practice, is out of the question since the segmentation leading by a surgeon or a radiologist using actual tools requires 6 to 8 hours.

Artificial Intelligence (AI) is a powerful tool capable of automatically performing image segmentation, but its performance is highly dependent on the quantity and quality of the data available. A knowledge approach helps to limit this dependence. In [16], we privileged the use of a CBR system coupled with a region growing algorithm, in order to perform kidney segmentation reached by a nephroblastoma. The main contribution of [16] was the adaptation of the seeds coordinates which ensured that they were well placed in the parenchyma of the pathologic kidney before starting segmentation. Despite the improvement in the results, the experiments highlighted the need to extend the adaptation step to the second type of parameters, namely thresholds, to avoid leakage phenomena that could severely deteriorate the accuracy of the yielded segmentations. In [15], we completed our work with a training method for CNN, but dedicated to the segmentation of nephroblastoma, called $OV^2ASSION$.

In this paper, we will first briefly present our platform dedicated to the segmentation of scanner images in children, COLISEUM-3D, before focusing on the CBR system for the segmentation of the pathological kidney. In particular, we will present a second adaptation dedicated to the threshold values used during segmentation by region growth so that the system itself is able to modify these values to find an optimal combination better adapted to the new problem.

2 Related work

Many methods exist for image segmentation and some are commonly used for medical applications. Huang *et al.* realized a recent and complete survey describing popular algorithms for breast tumour segmentation [10] . Thresholding is the simplest way to compute a segmentation but, as a histogram-based method, it is not very efficient for noisy images such as US images or CT-scans. Clustering is another classical method where pixels are divided into several groups and given feature vectors for each of them. Yet, results widely depend on initialization. Region-based methods such as watershed and region-growing algorithms have a similar problem. On the one hand, the watershed technique tends to produce over-segmentation because each basin in the image corresponds to a different region. In contrast, region-growing needs to be initialized with seeds. Most often, parameters are manually determined. Seeds and threshold values are respectively placed in the images and defined allowing to calculate a criterion to drive the regions growing. Mohammed *et al.* developed a process for automatic seed point selection in order to segment Nasopharyngeal Carcinoma (NC) from microscopy images, using probability maps [18]. Another way would be to enhance the region-growing process with Artificial Intelligence (AI). Despite its sensitivity to noise and a phenomenon of recurrent leakage, the region-growing algorithm is fast and efficient.

Many research studies relative to segmentation enhanced by AI using CBR ([19, 20, 5]), genetic algorithms ([6]), knowledge stored in ontologies ([3, 11, 23, 2]), Markov random fields ([12]) and Deep learning ([14]).

Though, in recent studies, Deep Learning appears to give the most accurate results. This technique requires a lot of data in order to be trained. In contrast, CBR gives an advantage to knowledge and enriches itself following its experiments ([13]). A large number of CBR systems designed for Health Science (CBR-HS) can be found in [1, 7–9, 17, 21, 22]. For instance, Saraiva *et al.* [22] designed a CBR and RBR (Rule Based Reasoning) system as a decision support system for diagnosis of gastrointestinal cancer. Petrovic *et al.* [21] worked on a CBR-HS to retrieve and adapt the best radiotherapy for patients. Gu *et al.* [7] realized a CBR system for diagnosis of breast cancer. In the image segmentation field, Perner [19] designed a system for segmentation of brain images with a cut histogram method. Frucci and Perner [5] adapted and improved this system with a watershed method. Burgos *et al.* [2] created another CBR system to retrieve the best segmentation process following the input images but for an agricultural application. This approach is inspired by Perner's one. Another interesting application was made by Ficet-Cauchard *et al.*. [4]. The architecture of an interactive system allows the user to use a set of freely selectable and configurable modules to perform a particular image processing task as image segmentation.

3 Materials and Methods

This part presents the material and method aspect of our work. A first section describes our COLISEUM-3D platform. Then, an overview of our CBR system for kidney segmentation is showed as a part of the platform. The main section concerns the update of the adaptation process for seeds position and especially for thresholds values.

3.1 COLISEUM-3D

COLISEUM-3D (**COL***laborative plateform with artificial* **I***ntelligence for* **SE***gmentation of t***U***moral kidney in* **M***edical images in* **3D**) is a platform dedicated to the segmentation of scanner images for the detection of different abdominal structures in children. The structures of interest are the parenchyma of the pathological kidney, the corresponding renal cavities, the nephroblastoma and the blood vessels (arteries and veins). The platform inputs are the different images of the patient to be segmented. These images can be taken in vascular time (when the contrast product is in the patient vessels) or in late time (when this contrast product is evacuated through the kideny cavities) depending on the structures of interest. Its output is a final and single segmentation of these structures. An overview of the platform is showed in Figure 1.

COLISEUM-3D is organized in layers, themselves made up of modules, as shown in Figure 1 and explained below:

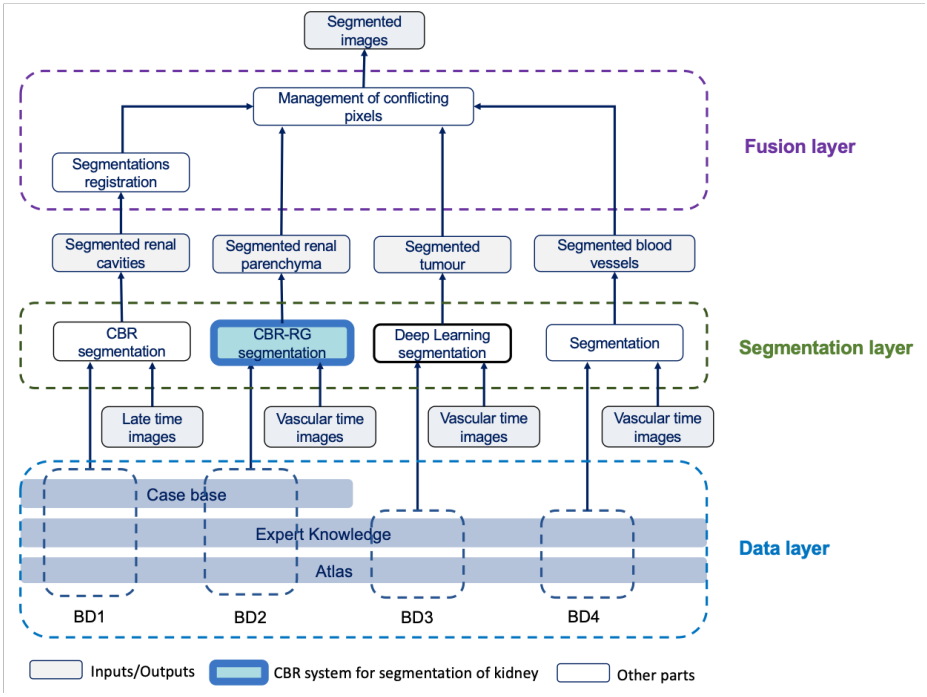

Fig. 1. Overview of COLISEUM-3D platform

– The data layer includes all the available data on which to base the solution of segmentation problems. It is itself divided into 3 sub-layers: the atlas, expert knowledge and the case base;
– The segmentation layer produces the different segmentations from the different inputs. It is composed of 4 distinct modules, each dedicated to the segmentation of a particular structure. Currently, a CBR system is used to segment the renal parenchyma and a Deep learning approach (presented in [15]) focuses on the segmentation of nephroblastoma;
– The fusion layer then merges the different segmentations in order to produce a single result. This involves label conflict resolutions.

3.2 CBR system for segmentation of pathologic kidney

Our system is an update of the one developed in our previous paper [16], dedicated to segmentation of renal parenchyma deformed by the presence of a nephroblastoma, and is presented in Figure 2. The input of the CBR system is a new CT-scan to segment. It searches in the case base the closer image already segmented (source case) for reuse its solution. For this search, It calculates a similarity value for each stored case and extracts the source case with the highest similarity during a retrieval phase. Then, extracted parameters of segmentation

are adapted to the current case through an adaptation phase. These adapted parameters are used to perform a new segmentation thanks to an region growing algorithm. Finally, the result is evaluated by an expert and stored in the case base as new source case if the segmentation is relevant.

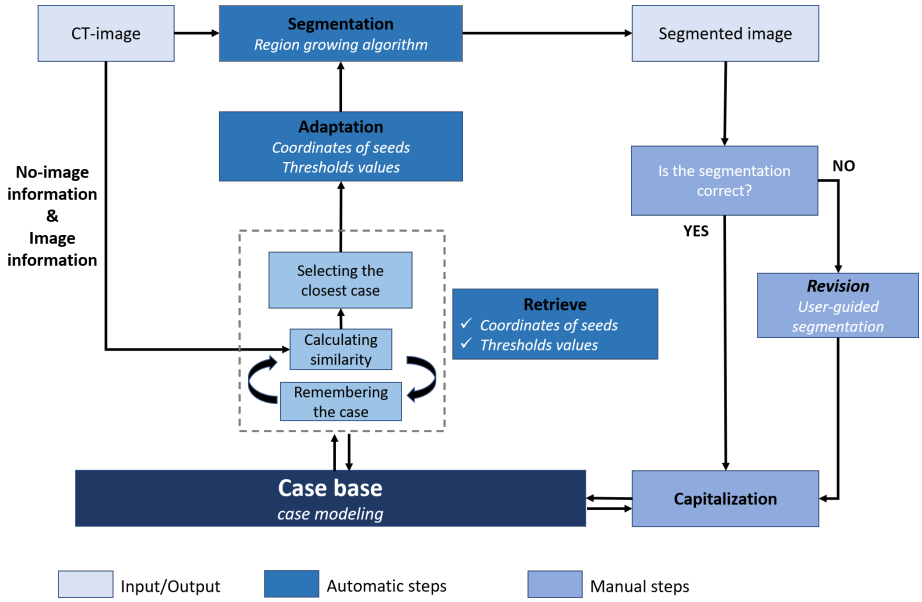

Fig. 2. Overview of our CBR system

Figure 3 describes the case structure. This case structure is an enhacement of the one used in the previous version of this tool and presented in [16]. The solution part is updated to take into consideration new criteria used during the new adaptation phase. In addition, we added the following items: intensity of seeds' pixels, area, centre of mass and orientation of segmentation.

$$Case = \begin{bmatrix} patient\ sex \\ patient\ age \\ patient\ height \\ patient\ weight \\ image\ mean \\ image\ kurtosis \\ image\ skewness \\ image\ variance \end{bmatrix} + \begin{bmatrix} list\ of\ pretreatments \\ 2D\ coordinates\ of\ kidney\ seeds \\ thresholds\ of\ kidney\ seeds \\ intensity\ of\ seeds'\ pixels \\ area\ of\ segmentation \\ centre\ of\ mass\ of\ segmentation \\ orientation\ of\ segmentation \end{bmatrix}$$

Description of problem part **Description of solution part**

Fig. 3. The case model of the CBR: problem part and solution part

3.3 Adaptation phase

The adaptation phase aims to automatically modify the parameters of regional growth in order to maximize the relevance of the result. According to the region growing algorithm presented in [16], there are two main types of parameters to be modified: the seed coordinates (used to initialize the algorithm) and the threshold values (controlling the propagation/growth of the regions). A modification of these parameters, even minimal, may infer big difference for the resulting segmentation. It is therefore paramount to achieve to create an adaptation phase robust enough in order to ensure the efficiency of the system. The number of seeds is never modified and the system only use the ones that come from the retrieval phase.

Adaptation of the coordinates of the seeds Part of the adaptation is to correctly place the seeds in the image. In [16], we suggested an algorithm to adapt the coordinates of the seeds. We automatically infered the correct position of seeds, considering the grey-level intensity I of the pixel and extenting step by step the neighborhood until finding it. We defined a coherence interval CI for each object to segment, corresponding to an interval of grey-level intensity a seed must be in, and a procedure to verify if a seed belongs to its dedicated region. This previous version outperformed a Level-Set technique (Dice equal to 75%) and FCN-8s (59%). In this work, we made some updates about the way we search the best position for seeds. First, we use a specific coherence interval CI for each retrieved seed in regards of a benchmark intensity i_{seed}. This value corresponds to the intensity of the pixel used to host the seed in the stored case. Secondly, the coherence interval CI is now dynamic around i_{seed} following an iteration value z. During a first step, the algorithm looks for a pixel with an exact intensity value i_{seed} in a window 50×50. If no position is found, the procedure starts from scratch by incrementing the value z. We limit the search of a better pixel intensity in a window in order to avoid seed placement in distant structures with an average intensity close from renal parenchyma. As a result, the test to verify the relevance of a seed position has changed as below:

$$\begin{aligned} \forall seed,\ isCorrectlyPlaced(seed) = true \ \ if \ \ I(seed) \in CI_{seed} \\ avec\ CI_{seed} = [i_{seed} - z, i_{seed} + z] \end{aligned} \tag{1}$$

Adaptation of the thresholds of the seeds As the region growth algorithm is very sensitive to initialization (different initial conditions have a lot of impact on the result), it is essential to adapt the position of the seeds. But this adaptation is not enough to guarantee the quality of the calculated segmentation and it is common that even with good coordinates, growth of seeds leads to an aberrant result. The problem is that the position adaptation does not prevent the leakage phenomenon in complex and sometimes low contrast images. If the location of the seeds plays a role in this, the sensitivity of the algorithm to this

phenomenon depends strongly on the threshold values used. The adaptation of the values of the thresholds aims at optimizing the values of 2 thresholds (local and global) per seed and determining an optimal combination. This implies designing a function that quantifies the quality of a segmentation (or the error) in order to maximize it (or respectively minimize it).

The evaluation criteria This function is based on 3 different criteria to characterize the calculated segmentation compared to the segmentation of the reference case. These 3 criteria correspond to the calculation of the first 3 geometrical moments. The geometrical moment of order ij, for an image in which each pixel has for coordinates (x, y) and for value $I(x, y)$, has for expression :

$$m_{ij} = \sum_x \sum_y x^i y^j I(x, y) \tag{2}$$

The first criterion m_{00} is the order time 0. In a segmentation in which the pixel values are binary (0 for the *background* and 1 for the segmented object), this is equivalent to calculating the area, in number of pixels, of the segmentation. Using Equation 2, we end up with :

$$m_{00} = \sum_x \sum_y I(x, y) \tag{3}$$

The second criterion is the center of mass, or center of inertia, C_m with coordinates $(\bar{x}, \bar{y})$:

$$\bar{x} = \frac{m_{10}}{m_{00}} \qquad \bar{y} = \frac{m_{01}}{m_{00}} \tag{4}$$

Finally, the third criterion θ allows to characterize the orientation of the segmentation in space :

$$\theta = \frac{1}{2} arctan\left(\frac{2m_{11}}{m_{20} - m_{02}}\right) \tag{5}$$

The score function In addition to these criteria, we have built a function *score* in order to evaluate the quality of a proposed segmentation. This function is itself composed of sub-functions calculating a score for each criterion :

$$scoreGlobal = (a * scoreSup + b * scoreCdM + c * scoreOrient)/(a + b + c) \tag{6}$$

Where *scoreSup*, *scoreCdM* and *scoreOrient* are the scores on the area criterion, the centre of mass criterion and the shape orientation criterion respectively. a, b and c are weight values that allow for the possibility, if necessary, of giving more weight to one criterion in relation to another in the calculation. Let x_{seg} be the x parameter calculated for the segmentation of the case to be solved and x_{ref} the parameter x obtained for the segmentation of the retrieved case. The scores are calculated by performing the difference $|x_{seg} - x_{ref}|$ and by standardizing them in order to delete the difference in scale of values between the 3 criteria.

Threshold adaptation algorithm In order to determine an optimal combination of parameters, we have defined the search intervals IR_{local} and IR_{global} around the reference thresholds $thresholdLocal_{ref}$ and $thresholdGlobal_{ref}$ such that:

$$\begin{aligned} IR_{local} &= [thresholdLocal_{ref} - \alpha, thresholdLocal_{ref} + \alpha] \\ IR_{global} &= [thresholdGlobal_{ref} - \alpha, thresholdGlobal_{ref} + \alpha] \end{aligned} \tag{7}$$

where α is a value to control the extent of the search. In order to limit the complexity of the problem, we have used a maximum of 3 seeds to initiate the segmentation. We have favored a heuristic approach that allows us to efficiently explore a small part of the possibilities in order to obtain an acceptable solution, i.e. one that can be medically exploited. We have used the DICE and IU indices in order to validate the segmentations obtained in relation to the manual segemtation done by physicians.

Algorithm 1 proceeds by several stages for adapting the thresholds. First of all, the *seg* segmentation is calculated a first time with the list of seeds *lseeds* directly from the retrieval process. This provides the initial score as a basis for finding a better combination of thresholds. The score calculation uses the weights a, b and c as defined in Equation 6. They must be defined empirically to maximize the quality of the segmentations. Indeed, modifying these weights impacts the different criteria (area, center of mass and orientation) in the definition of a optimal segmentation and therefore modifies the results of the CBR system. For each seed of the *lseeds*, all possible pairs $(threshold_{local}, threshold_{global})$ are explored, in accordance with the following search intervals α, by setting the other values and then the segmentation produced by each of them is evaluated. If the score of the new segmentation is higher than that of the previous one, the new threshold values are retained, otherwise, the old values are reassigned. The algorithm returns the list of seeds, with adapted thresholds to the current problem.

4 Results

This section presents our experimentations and the results obtained. The first part presents the way the experimentations have been performed. The second part shows our results for the determination of the best combinaison of weights for thresholds adaptation and hightlights the interest of our adaptation phase in the CBR system. Finally, the segmentations obtained with this CBR system are compared to the ones obtained with a CNN in the lart part of this section.

4.1 Database, initial hypothesis and conditions, and evaluation process

In order to evaluate the second stage of adaptation (modification of thresholds), the experiments are based on a database of 33 CT-scans segmented using a

Algorithm 1 Adaptation of seeds threshold values

Require: $image$, $lseeds$, $infoSeg_{ref}$, α, a, b, c
Ensure: $lseeds$
  $seg \leftarrow segmentation(image, lseeds)$
  $scoreArea \leftarrow calculScoreArea(seg, infoSeg_{ref}.area)$
  $scoreCoM \leftarrow calculScoreCoM(seg, infoSeg_{ref}.centerOfMasse)$
  $scoreOrient \leftarrow calculScoreOrient(seg, infoSeg_{ref}.orientation)$
  $scoreGlobal \leftarrow a * scoreArea + b * scoreCoM + c * scoreOrient$
  for each seed s of $lseeds$ **do**
    $localThreshold_{ref} \leftarrow s.localThreshold$
    $globalThreshold_{ref} \leftarrow s.globalThreshold$
    for i from $-\alpha$ to α **do**
      for j from $-\alpha$ to α **do**
        $localThreshold_{temp} \leftarrow s.localThreshold$
        $globalThreshold_{temp} \leftarrow s.globalThreshold$
        $s.localThreshold \leftarrow localThreshold_{ref} + i$
        $s.globalThreshold \leftarrow globalThreshold_{ref} + j$
        $seg \leftarrow segmentation(image, lseeds)$
        $scoreArea \leftarrow calculScoreSup(seg, infoSeg_{ref}.area)$
        $scoreCoM \leftarrow calculScoreCdM(seg, infoSeg_{ref}.centerOfMasse)$
        $scoreOrient \leftarrow calculScoreOrient(seg, infoSeg_{ref}.orientation)$
        $scoreGlobal_{new} \leftarrow a * scoreArea + b * scoreCoM + c * scoreOrient$
        if $scoreGlobal_{new} > scoreGlobal$ **then**
          $scoreGlobal \leftarrow scoreGlobal_{new}$
        else
          $s.localThreshold \leftarrow localThreshold_{temp}$
          $s.globalThreshold \leftarrow globalThreshold_{temp}$
        end if
      end for
    end for
  end for
  return $lseeds$

region growth manually guided by an expert, giving as many different cases. The cases are extracted from the examinations of 3 different patients, which we will name here respectively P1, P2 and P3. Table 1 summarizes the information on the constitution of this base. Note that we limit ourselves here for each patient to the sections in which the pathological kidney is present. Therefore, it does not refer to the entire examination. Finally, we have 33 images used to build the case base and 150 images to evaluate the system.

In order to improve the quality of the calculated segmentations, post-processing was applied to the images output from the CBR system. The renal parenchyma being organized in 2 distinct tissues, the cortex and the medulla. Actually, surgeons did not distinguish these 2 tissues during their segmentations considered as ground truth. But the region growth algorithm distinguished them sometimes. The post-processing consists of therefore applying a filling algorithm in order to merge these 2 structures in one.

	Nb of images	Nb of images in the base	Nb of tested images
P1	40	12	28
P2	55	13	42
P3	88	8	80
Total	183	33	150

Table 1. Case base for evaluation of our CBR system

4.2 Determination of optimal weights

The threshold adaptation step uses an overall score so that the system is able to assess the relevance of a segmentation associated with a combination of threshold values. The expression for the global score was given by Equation 6. It uses a set of 3 weights a, b and c determining the influence of each criterion in the calculation. The determination of these weights is empirical. In this part, we experiment the adaptation of the threshold values for the seeds, according to Algorithm 1, with different triplets (a, b, c).

Four versions of the adaptation algorithm called respectively AdaptV0, AdaptV1, AdaptV2 and AdaptV3 are evaluated and faced to the lack of adaptation :

AdaptV0 Algorithm with adaptation of seeds positions only.
AdaptV1 Algorithm with a triplet weight (1,0,0).
AdaptV2 Algorithm with a triplet weight (a,b,c) without nomalization.
AdaptV3 Algorithm with a triplet weight (a,b,c) with nomalization.

Table 2 presents the results obtained for patients P1, P2 and P3 indicating, Dice scores for each of them. The score is determined for a patient at one time by considering the whole examination as one and the same 3D image. This method gives more relevant results than average because it is free from a calculation bias that can artificially decrease or increase the score. A large number of weight combinations was tested during the experiments but only the results of a sample of these combinations are presented. Without adaptation, we obtained a Dice score from 0.245 to 0.543. An adaptation of seed position only succeeded to significantly improve the performances for all patients. This improvement increases with a fully adaptation step. AdaptV1 achieves Dice index between 0.817 and 0.867 . The introduction of 2 additional criteria by AdaptV2 allows to have a clear improvement. AdaptV3 corresponding to a willingness to correct a methodological bias in the calculation of the criteria by standardizing them between 0 and 1. The best results are achieved for the triplet $(20, 10, 1)$ enabling a better mean segmentation accuracy for patients P1 and P3. These results also show that it is difficult to find an optimal (a, b, c) weight triplet for all patients. Some triplets may give the best result on one and the worst on another. The $(20, 10, 1)$ triplet appears to be the most relevant here because it provides good segmentations on all patients tested, but it is likely to lose relevance on others.

	NoAdapt	**AdaptV0**	**AdaptV1**	**AdaptV2 (1,150,4500)**	**AdaptV3 (1,1,1)**	**AdaptV3 (8,2,1)**	**AdaptV3 (20,10,1)**
P1	0.455	0.620	0.826	0.826	0.651	0.806	0.830
P2	0.245	0.319	0.817	0.824	0.816	0.827	0.824
P3	0.543	0.712	0.867	0.888	0.899	0.882	0.897

Table 2. Global Dice measures obtained by the region growth segmentations guided by our CBR system with adaptation of the seeds positions and thresholds.

Figure 4 highlights the importance of this new adaptation phase in our CBR system, as well as its effectiveness, with a series of examples. For the 4 images presented, the system failed to correctly segment the renal parenchyma when the threshold adaptation is missing (which corresponds to the previous version of this CBR [16]). For these 4 cases, the activation of the adaptation phase significantly increased the quality of the result, even if it did not manage to produce a perfect segmentation.

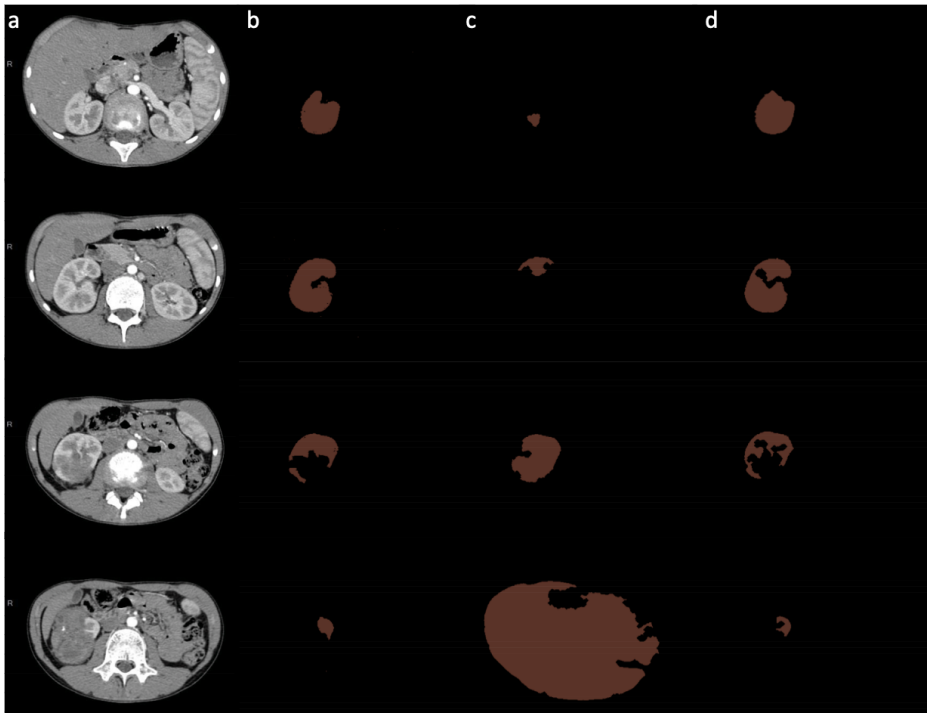

Fig. 4. Results of the region growth segmentation of different CT-scans (a) : (b) ground truths (c) without threshold adaptation (d) with threshold adapation using triplet (20,10,1)

4.3 Comparaison with $OV^2ASSION$ approach for segmentation of tumoral kidneys

We have finally compared the segmentations obtained by CBR system (with its complete adaptation phase) to the ones obtained using a CNN (FCN-8s), trained according to our $OV^2ASSION$ method from [15], for the segmentation of the pathological renal parenchyma. The interest is that this method places the CNN in a favorable situation (segmentations to be calculated close to those included in the learning set LS) and optimizing the segmentation accuracies. The case base of the CBR system is identical to that of the previous experiments. The same patients P1, P2 and P3 have been used for these tests. We have used CBR with its complete adaptation phase (seeds' coordinates and threshold values), with the weight combination $(20, 10, 1)$. To perform the comparison under similar conditions, we set up the method $OV^2ASSION$ with a gap $g = 4$ and a vector $(V_4)_1$. The constitution of both of the databases is presented in Table 3. Only the number of data for P3 is significantly different (twice as many important for FCN-8s).

	Total Nb of images	**Nb of images case base of CBR**	**Nb of images learning set of FCN-8s** ($g = 4$)
P1	40	12	8
P2	55	13	11
P3	88	8	18

Table 3. Contents of the databases for CBR and FCN-8s

Table 4 presents the scores of Dice and IoU of both approaches, calculated only on missing images on the bases. For all patients, the CBR system is reached, thanks to its adaptation phase, to calculate segmentations more accurate than those proposed by FCN-8s. Both of the systems deliver performance very close for P3 with an advantage in favour of the CBR system. The pathological kidney of P3 has a healthy appearance on a large number of slices, this may explain why the CNN also manages to give good results. However, CBR keeps a superior performance while relying on a weaker database than FCN-8s (8 images versus 18).

5 Discussion and future work

Our results showed that our CBR system could significantly improve the accuracy of kidney parenchyma segmentation with a region growing algorithm, despite strong deformations induced by the presence of nephroblastoma. These good results are strongly linked to the existence of an adaptation of the seeds

	RàPC-CR with full adaptation		**FCN-8s** $OV^2ASSION$ $g = 4$	
	Dice	**IoU**	**Dice**	**IoU**
P1	0.830	0.710	0.763	0.617
P2	0.824	0.700	0.729	0.574
P3	0.897	0.814	0.881	0.788

Table 4. Comparison of Dice and IoU scores for the segmentation of renal parenchyma (pathological) between our CBR system (with full adaptation) and FCN-8S trained according to the $OV^2ASSION$ method

positions and thresholds. This one allows first of all to improve the likelihood that the seeds are properly placed and ensure better threshold values to lead the segmentation despite the small size of data base which is a medical constraint we have to deal with. A performance comparison when this adaptation is activated or disabled has clearly highlighted this contribution. On the other hand, the CNN showed poorer performance under the same conditions despite an advantageous situation allowed by the $OV^2ASSION$ method. The main limitation of the current system, however, remains the small size of the case base, which cannot be fully compensated for by adaptation. Of course, this limitation becomes all the more problematic when the kidney of the considering patient is of an original (unexpected) aspect (considering the system case-base). Beyond the question of a novel shape/position of the tumour (and therefore of the kidney by extension), there is also the problem of the laterality of the nephroblastoma. There are situations in which the characteristics of the kidney to be segmented may be very close to a stored case, which should logically lead to a relevant segmentation, but for which the pathological kidney is on the other side in this new target problem in relation to this stored case. This then leads to an inability of the system to compute a correct segmentation when all the conditions are met. The consequence is an under-exploitation of the knowledge available by the system, implying the need to complete the case base to maintain its efficiency and to predict the mirror cases. If we add the fact that including new cases is very time-consuming, the optimal exploitation of this knowledge is an essential point to work on. The relevance of the scoring criteria used for the adaptation of the thresholds, namely area, center of mass and orientation of the segmented form, should also be questioned. These criteria appear to be very interesting to describe the image but they are insufficient in use to guarantee the convergence of the algorithm towards the best possible segmentation. Thus, determining the weights to be given for each of these criteria remains an area of improvement.

Other futur works will be considered in order to improve this CBR system results. First, the determined weights are the best for the tested data but there is no guarantee there are for all patients. Further experimentations are required in order to optimize these weight values. For example, the combinaison of weights (a, b, c) could be also integreted in the case solution. Second, our adaptation step

does not allow all the differences between the stored cases and the new cases to be solved. It would be interesting to be able to design a modular adaptation capable of building an original solution from several different solutions stored in the database according to the relevance of their different parts.

6 Conclusion

The core of this work has enabled us to propose a segmentation solution by AI to extract the renal parenchyma from CT-scans, with the important lock of the limited amount of data available. This solution uses a Case Based Reasoning (CBR) system to guide a region growth algorithm. In particular, we have imagined an adaptation phase for the main intialization parameters of such an algorithm, namely the seed coordinates and the threshold values. We were able to demonstrate the efficiency of this adaptation and the clear improvement of performance induced. The presence of this adaptation has strongly limited leakage phenomena, which are common when a segmentation by growth of regions is performed. This adaptation has also increased the probability of segmenting the desired structure by correctly placing the seeds in the image.

Acknowledgements

The authors wish to thank Pr Frédéric Auber, Dr Marion Lenoir-Auber and Dr Yann Chaussy of the *Centre Hospitalier Régional Universitaire de Besançon* for their expertise with nephroblastoma and for achieving the manual segmentations with help of Loredane Vieille. The authors thanks *European Community* (*European FEDER*) for financing this work by the *INTERREG V*, the *Communauté d'Agglomération du Grand Besançon* and the *Cancéropôle Grand-Est.*

References

1. Attig, A., Perner, P.: Incremental learning of the model for watershed-based image segmentation. In: Combinatorial Image Analaysis, pp. 209–222. Springer (2012)
2. Burgos-Artizzu, X.P., Ribeiro, A., Tellaeche, A., Pajares, G., Fernández-Quintanilla, C.: Improving weed pressure assessment using digital images from an experience-based reasoning approach. Computers and electronics in agriculture **65**(2), 176–185 (2009)
3. Colliot, O., Camara, O., Bloch, I.: Integration of fuzzy spatial relations in deformable models—application to brain mri segmentation. Pattern recognition **39**(8), 1401–1414 (2006)
4. Ficet-Cauchard, V., Porquet, C., Revenu, M.: Cbr for the reuse of image processing knowledge: a recursive retrieval/adaptation strategy. In: International Conference on Case-Based Reasoning. pp. 438–452. Springer (1999)
5. Frucci, M., Perner, P., di Baja, G.S.: Case-based reasoning for image segmentation by watershed transformation. In: Case-Based Reasoning on Images and Signals, pp. 319–353. Springer (2008)

6. Golobardes, E., Llora, X., Salamó, M., Martı, J.: Computer aided diagnosis with case-based reasoning and genetic algorithms. Knowledge-Based Systems **15**(1), 45–52 (2002)
7. Gu, D., Liang, C., Zhao, H.: A case-based reasoning system based on weighted heterogeneous value distance metric for breast cancer diagnosis. Artificial intelligence in medicine **77**, 31–47 (2017)
8. Henriet, J., Lang, C.: Introduction of a multiagent paradigm to optimize a case-based reasoning system designed to personalize three-dimensional numerical representations of human organs. Biomedical Engineering: Applications, Basis and Communications **26**(05), 1450060 (2014)
9. Henriet, J., Leni, P.E., Laurent, R., Salomon, M.: Case-based reasoning adaptation of numerical representations of human organs by interpolation. Expert Systems with Applications **41**(2), 260–266 (2014)
10. Huang, Q., Luo, Y., Zhang, Q.: Breast ultrasound image segmentation: a survey. International journal of computer assisted radiology and surgery **12**(3), 493–507 (2017)
11. Hudelot, C., Atif, J., Bloch, I.: Fuzzy spatial relation ontology for image interpretation. Fuzzy Sets and Systems **159**(15), 1929–1951 (2008)
12. Kato, Z., Zerubia, J., et al.: Markov random fields in image segmentation. Foundations and Trends® in Signal Processing **5**(1–2), 1–155 (2012)
13. Kolodner, J.: Case-based reasoning. Morgan Kaufmann (2014)
14. Litjens, G., Kooi, T., Bejnordi, B.E., Setio, A.A.A., Ciompi, F., Ghafoorian, M., van der Laak, J.A., van Ginneken, B., Sánchez, C.I.: A survey on deep learning in medical image analysis. Med Image Anal **42**, 66–88 (Dec 2017)
15. Marie, F., Corbat, L., Chaussy, Y., Delavelle, T., Henriet, J., Lapayre, J.C.: Segmentation of deformed kidneys and nephroblastoma using case-based reasoning and convolutional neural network. Expert Systems with Applications **127**, 282–294 (2019)
16. Marie, F., Corbat, L., Delavelle, T., Chaussy, Y., Henriet, J., Lapayre, J.C.: Segmentation of kidneys deformed by nephroblastoma using case-based reasoning. In: International Conference on Case-Based Reasoning. pp. 233–248. Springer (2018)
17. Marling, C., Montani, S., Bichindaritz, I., Funk, P.: Synergistic case-based reasoning in medical domains. Expert systems with applications **41**(2), 249–259 (2014)
18. Mohammed, M.A., Ghani, M.K.A., Hamed, R.I., Abdullah, M.K., Ibrahim, D.A.: Automatic segmentation and automatic seed point selection of nasopharyngeal carcinoma from microscopy images using region growing based approach. Journal of Computational Science **20**, 61–69 (2017)
19. Perner, P.: An architecture for a cbr image segmentation system. Engineering Applications of Artificial Intelligence **12**(6), 749–759 (1999)
20. Perner, P.: Why case-based reasoning is attractive for image interpretation. In: Case-based reasoning research and development, pp. 27–43. Springer (2001)
21. Petrovic, S., Khussainova, G., Jagannathan, R.: Knowledge-light adaptation approaches in case-based reasoning for radiotherapy treatment planning. Artificial intelligence in medicine **68**, 17–28 (2016)
22. Saraiva, R., Perkusich, M., Silva, L., Almeida, H., Siebra, C., Perkusich, A.: Early diagnosis of gastrointestinal cancer by using case-based and rule-based reasoning. Expert Systems with Applications **61**, 192–202 (2016)
23. Trzupek, M., Ogiela, M.R., Tadeusiewicz, R.: Intelligent image content semantic description for cardiac 3d visualisations. Engineering Applications of Artificial Intelligence **24**(8), 1410–1418 (2011)